High-repetition rate LWFA system in Gemini Target Area 2

Contact *kirill.fedorov@stfc.ac.uk*

K. Fedorov, D. R. Symes, C.D. Armstrong, S, Devadesan, O. Finlay, S. J. D. Dann, C. Selig, B. Spiers, N. Bourgeois, T. Dzelzainis. W. Robins, Z. Athawes-Phelps, R. Sarasola, D. Bloemers, I. Symonds, B. Morkot, A. Thomas, R. Lyon, T. Pocock.

Central Laser Facility
STFC Rutherford Appleton Laboratory
Harwell Campus, Didcot, OX11 0QX, UK

A. Gunn

The John Adams Institute for Accelerator Science,
Imperial College London,
London SW7 2AZ, UK.

T. Pacey, Y. Saveliev, S. Mathisen

The Cockcroft Institute, Accelerator Science and Technology Centre, STFC Sci-Tech Daresbury, Warrington WA4 4AD, UK

A. Bhardwaj, R. Sugumar

Indian Institute of Technology Hyderabad,
Kandi, Telangana, 500046,
India

1 Introduction

Gemini Target Area 2 (TA2) has been closed for open application in order to carry out R&D necessary for prototyping and delivering EPAC [1]. In this report, we describe elements of the experimental setup that have been developed for this purpose, including the laser beamline and diagnostics, electron beam diagnostics, and available LWFA manipulation mechanisms. We emphasize that while these activities are led by the facility, we are fully collaborating with our user community at all stages.

The arrangement for laser wakefield acceleration will be based on a previous experiment in TA2 led by the John Adams Institute at Imperial College [2]. This demonstrated the application of Bayesian optimization to LWFA (subsequently also achieved at DESY [3]) operating at 1 Hz. As shown in Fig. 1, the target chamber and diagnostics chamber were surrounded by shielding suitable for a high repetition rate experiment. With dielectric gratings installed in the compressor, we should be able to increase the repetition rate to 5 Hz. Further experiments with machine-learning algorithms should allow us to find robust, stable operating conditions [4]. Our aim is to produce 10 pC bunches with <5% energy spread at 100 MeV, with both good shot-to-shot and long-term stability.

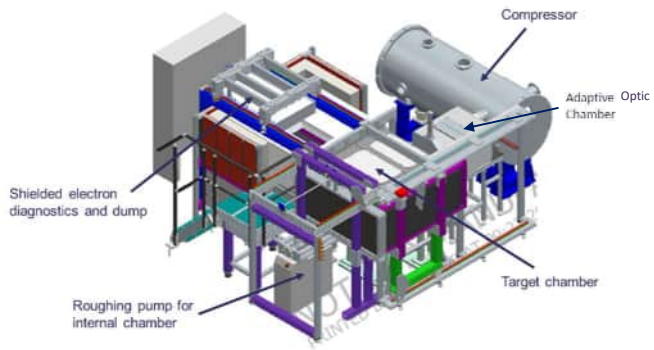

Figure 1. Experimental arrangement in TA2 for producing high repetition rate 100 MeV electron beams.

One of the key advances of EPAC will be to progress from experimental research to providing a fully functioning LWFA beamline suitable for applications. It is important to understand what mechanisms require controlling, and how to effectively manipulate the electron beam. The ability to manipulate the 6-D phase space (x,p_x,y,p_y,z,p_z) of a beam is critical to meet the demands of various applications. For instance, in conventional accelerators, longitudinal magnetic compression is used to achieve high peak current and to tune longitudinal profile (z). Momentum (p_z) can be manipulated by an accelerating cavity, whereas transverse emittance (x,p_x,y,p_y) is determined by the magnetic lattice structure. To prevent longitudinal beam deterioration, the technique of longitudinal-to-transverse (z-x/y) beam emittance exchange is utilized, as it is also capable of increasing collision luminosity. In the case of LWFA, the reduction in the overall length of the accelerators already opened the possibility for wider use of such machines, however classical beam manipulation techniques are often incompatible due to the compactness and ultra-short nature of the electron bunches.

Construction of the TA2 LWFA beamline will allow us to test components and develop new techniques in an iterative way that is not possible during short access slots on an operational user facility. We aim to continue studies of beam optimization through manipulation of a variety of factors, including plasma density, acceleration length, and laser pulse shape. Through this work, we aim to demonstrate robust control code that can apply automation and machine-learning to EPAC operations. With a stable beamline we will also be able to test magnetic focusing systems and femtosecond bunch diagnostics, and assess the impact of laser beam dumps on the electron beam quality.

2 Laser System in Gemini TA2

TA2 has been significantly remodeled for the forthcoming experimental campaign, aiming to provide a stable, high energy laser beam to an interaction with a gas target. Figure 2 shows a detailed description of the main beam path and diagnostic layout. The beam delivered from Gemini Laser Area 2 has energy 1 J in a 500ps pulse operating at up to 5Hz. Upon entry to the target area, this is split into a main beam, containing 95% of the energy, and a probe beam, derived from a 5% leakage through a turning mirror. On the path to the target chamber, the main beam also provides a further 1% energy leakage to both the pre- and post-compressor diagnostics. These are equipped with a near-field monitor, a far-field monitor and a wavefront sensor (Imagine Optic HASO), making a daily re-alignment routine straightforward, as well as providing a set of comprehensive references for potential single shot measurements. The final diagnostic for the main laser beam is a focal spot camera installed inside the target chamber after an $f/18$ (1 m focal length) off-axis parabola. The recent installation of multi-layer dielectric (MLD) gratings increases the energy throughput of the

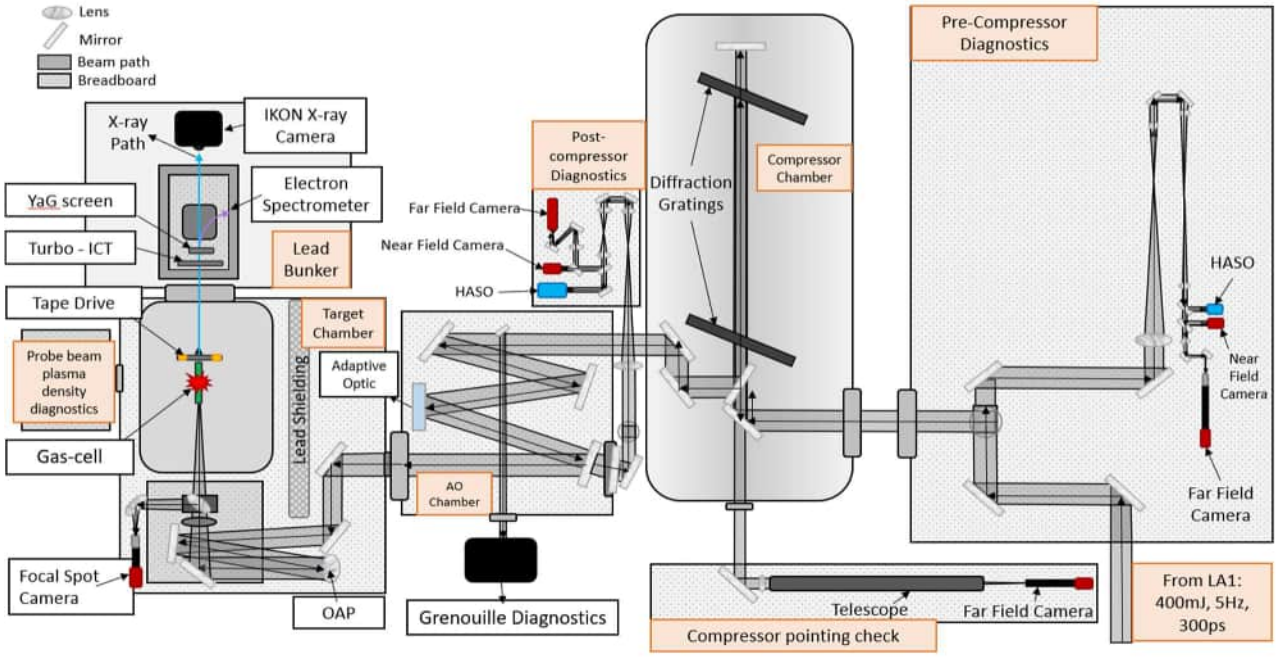

Figure 2. Schematic for Gemini TA2 laser beamline, diagnostics, compressor, and target interaction chamber.

compressor and is also expected to eliminate the compressor deformation caused by heating of gold gratings [1].

The temporal and spatial shape of the laser pulse on target can be controlled through an acousto-optic modulator (Fastlite Dazzler [5]) and a CLF-built piezo-electric adaptive optic (AO). Using these, secondary source properties can be tailored using optimization feedback strategies [2].

2.1 Characterisation of laser performance

Wavefront Optimization

The TA2 adaptive optic is located in a separate chamber (see Fig. 2) after the compressor and before a set of turning mirrors onto the parabola in the target chamber. This optic is used for initial optimisation of the post-compressor wavefront to correct aberrations from the laser system and produce the best focal spot-on target (at interaction point) on a daily basis. The adaptive optic can subsequently be used in a feedback system to stabilize the focal plane position, and to add aberrations intentionally in an optimization loop. The wavefront is optimized using the WaveTune software by Imagine Optic [6]. Figure 3 shows images of the wavefronts collected with the pre-compressor and post-compressor HASO sensors and corresponding far-field images. Note that astigmatism presented in pre-compressor and post-compressor far field has been corrected with the AO to achieve the best focal spot at the interaction point. The focal spot achieved with the $f/18$ parabola ($1/e^2$ of 16μm) at the interaction point is also shown in Fig. 3.

TA2 Operational Stability

The stability of the laser is critical to achieving high quality electron beam performance. Using large datasets, correlations between laser properties and electron energy can be determined [7, 8]. Our first task is to characterize the laser beam on short and long timescales and then implement both passive and active stabilization schemes. Drifts are relatively straightforward to deal with using motorized mirrors, lenses, the adaptive optic, and waveplate energy

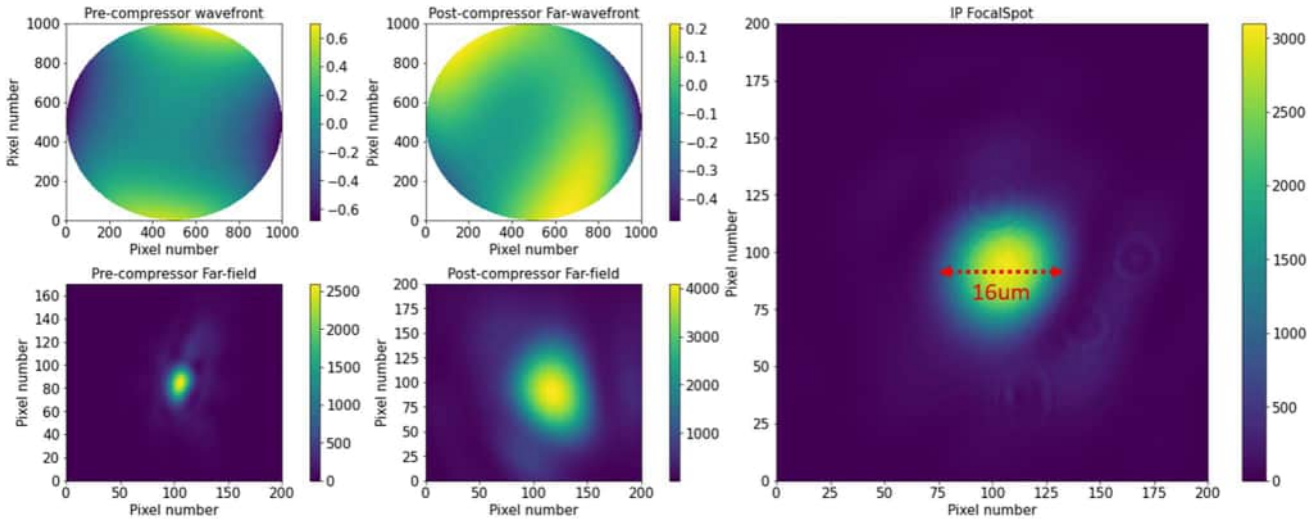

Figure 3. LEFT: Pre-compressor wavefront and corresponding far-field image; MIDDLE: Post-compressor wavefront and corresponding far-field image; RIGHT: Focal spot at the interaction point.

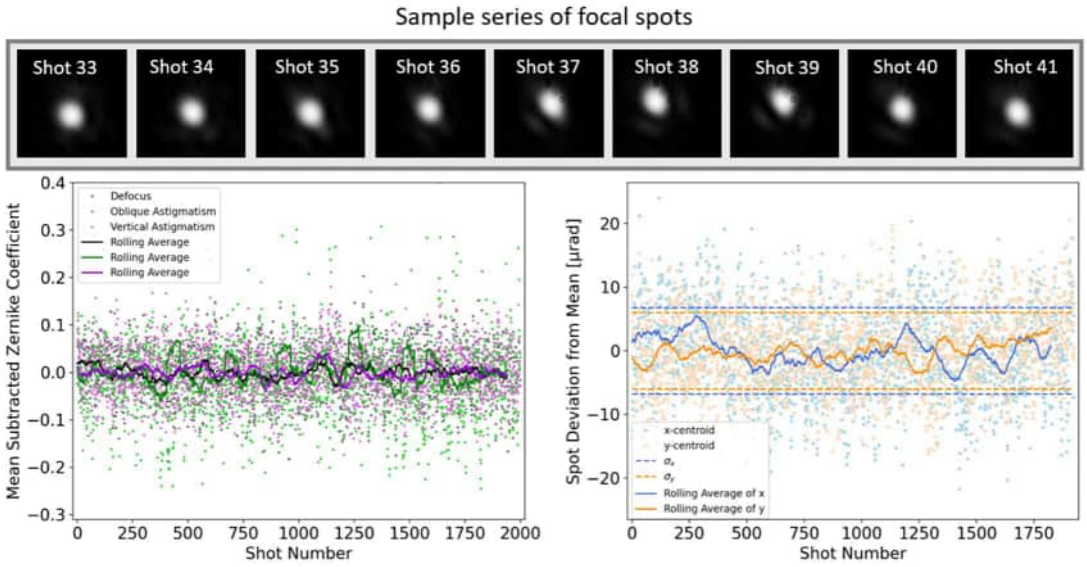

Figure 4. TOP: Sample series of focal spot images. LEFT: Three Zernike coefficients throughout the test scan, plotted as mean subtracted values with rolling averages. The colours correspond as follows: pink – vertical astigmatism; green – oblique astigmatism; grey – defocus. RIGHT: The x (blue) and y (orange) mean subtracted centroid values of the focal spot over the test scan, plotted with rolling averages and ± one average standard deviation for each axis.

control [3]. Shot-to-shot jitters are more difficult, and we do not anticipate tackling these in TA2, however due to the suite of on-shot diagnostics we will be able to monitor any unexpected motion.

We carried out a preliminary measurement of the laser stability by recording the centroid position of the focal spot, and the Zernike coefficients over a test run of 2000 shots (400 seconds). The data from the post compressor near field camera and HASO wavefront sensor, shown in Fig. 4, demonstrates the fluctuation of the parameters over this time. Further work is needed to analyze characteristic frequencies to determine correlations with environmental conditions, and to install feedback systems.

2.2 TA2 real-time visualization system

Daily operation of TA2 at 5Hz requires active monitoring of various laser parameters to assess short and long-term stability of the system. To achieve this, we developed a toolkit for real-time live-plotting and analysis of acquired data from the data servers. Figure 5 demonstrates the GUI deployed in the TA2 control room performing single-shot monitoring of pre-compressor and post-compressor near-field (NF), far-field (FF), and wavefront (a-f), long-term monitoring of wavefront Zernike coefficients (g,h), energy derived from the near-field (i,j), and far-field pointing (k,l). During further work all necessary LWFA parameters will be included.

3. LWFA Diagnostics

Diagnostics for LWFA [9] mirror those used in conventional RF accelerators. The main challenges for LWFA are the need to measure the ultra-short duration (a few fs) and the ultra-small normalized transverse emittance ($\varepsilon_n < 0.1$ mm mrad) of plasma-accelerated electron bunches. These are all required to be measured during a single-shot due to fluctuations in laser and plasma parameters.

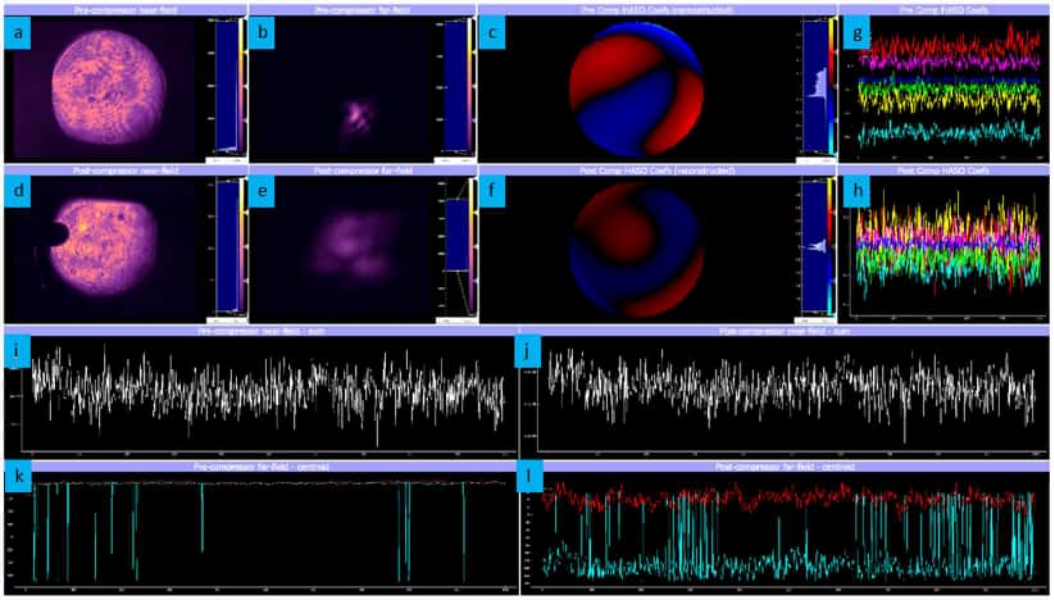

Figure 5. Live-plotting system in TA2 control room: a) pre-comp NF; b) pre-comp FF; c) pre-comp wavefront; d) post-comp NF (shadow from Grenouille diagnostic pick-off mirror (see Fig. 2); e) post-comp FF; f) post-comp wavefront; g) pre-comp Zernike coefficients; h) post-comp Zernike coefficients; i) pre-comp energy; j) post-comp energy; k) pre-comp pointing; l) post-comp pointing. Screenshot was taken during a grating heating test (November 2023).

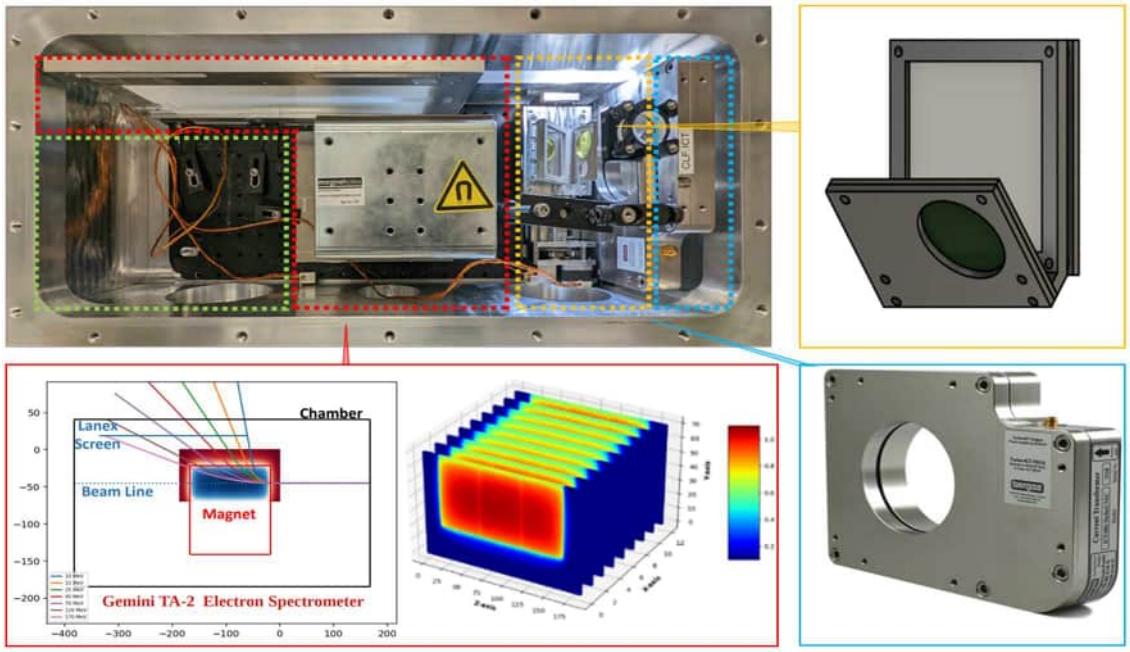

Figure 6. The diagnostics chamber, developed to house specific diagnostics, colour coded as follows: green – space reserved for CT sample; red – electron spectrometer; orange – the YAG:Ce screen; blue – Bergoz turbo-ICT.

Using TA2 we aim to test crucial diagnostics that we are planning to field on EPAC:

- Turbo-ICT capable of measuring short electron bunches
- YAG:Ce screen and imaging system for high resolution transverse e^--beam profile measurements
- High frame rate data acquisition for CT scans

The design of the chamber that is used to house these diagnostics is shown in Fig. 6. We will also investigate novel diagnostic techniques, such as longitudinal profile diagnostics exploiting a dielectric streaker, THz beam position monitors, emittance measurement using permanent quadrupoles, and electron spectrum measurements using the Cherenkov effect in fibre [10].

3.1 Integrated Current Transformer (Turbo-ICT) for Electron Beam Charge Measurement

Precise, single-shot, non-destructive charge measurements ($Q = N_e \cdot e$), where N_e - number of electrons, e – electron charge, of nano-coulomb particle bunches produced by EPAC is important for beam monitoring both for industrial and scientific applications. A conventional approach for single-shot electron bunch charge measurements is the use of a Faraday cup. However, this is a destructive method, and becomes bulky when using energies up to the GeV level where a large stopping distance is required. Another approach is the use of calibrated scintillator screens, though the signal depends on the energy and therefore needs to be cross-referenced with an electron spectrometer, which is, for example, not possible to provide just after the gas-cell (see Fig. 7). The common choice presently is to use an integrated current transformer (ICT), which measures the integrated current that a bunch of electrons induce in a coil upon passing through it.

The Turbo-ICT has several potential sources of instabilities and noise, which will be investigated in TA2 prior to its use in EPAC. For example, background from strong electro-magnetic pulses (EMP) generated during laser-plasma interactions, and non-relativistic electron clouds which accompany LWFA electrons. During testing in TA2, we will cross-reference the ICT with a calibrated Gadox screen (e-spec) or Faraday cup.

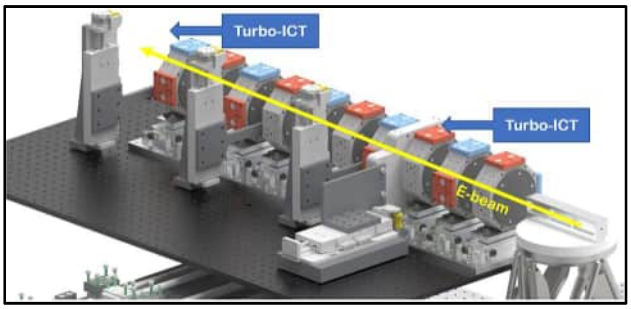

Figure 7. Bunch charge diagnostics for EPAC. A pair of Bergoz Turbo-ICT in use to monitor charge in two positions: emitted from the gas target and delivered to the interaction point.

The Turbo-ICT system from Bergoz Instrumentation [11, 12] has a readout compatible with the EPICS [13] control system used throughout EPAC. Thus, the measurements can be used as an objective function for algorithms optimizing charge through control of the laser and plasma properties [2, 14].

3.2 YAG Screen for Electron Beam Transverse Profile Diagnostics

One of the main parameters of an electron beam is the transverse profile. At EPAC, this will be used to measure the beam emittance (volume occupied by the beam in phase space), and to optimize both the beamline (Halbach quadrupoles layout) operation and the event rate of any collision process, such as Inverse Compton Scattering [15]. Cerium-doped YAG (YAG:Ce) is an effective scintillation material, and is also more suitable for fine diagnostics than Gadox, as it avoids a grain-size resolution limit. The resolution capability of Gadox varies from 40 - 80 μm [16] for "fine" and "medium" grain respectively. Better resolution between the two screens corresponds to a reduction in thickness from 140 to 70 μm. Meanwhile, YAG:Ce can provide a resolution limit as low as 10 μm for a 100 um thick crystal [17]. The overarching aim of these works for EPAC is optimising beam delivery, therefore the resolution will be prioritized over other parameters. In this manner, TA2 will be fitted with a YAG:Ce screen assembly (Fig. 6), which will provide a photon yield of $30 \cdot 10^3$ Ph per MeV deposited, with

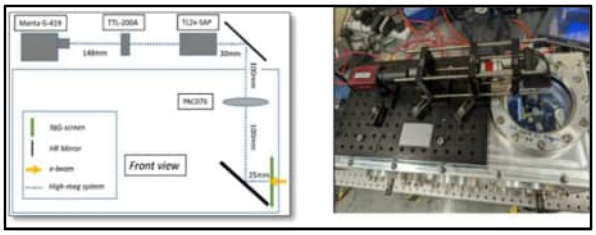

Figure 8. YAG screen high-magnification imaging system.

reported afterglow of <0.005 % at 6ms [17]. The assembly includes a calibration reticule, which allows for fine and easy alignment of the imaging system. It is positioned on translation stage to allow for:

- electron interactions with the YAG screen
- calibration reticule observation
- free-pass for electrons

This assembly will allow us to achieve a resolution of 6µm (161.3 line pairs/mm – group 7, element 3), meaning that the restricting factor in the imaging system is the YAG:Ce grain resolution limit (Fig. 9).

Figure 9. Images of USAF 1951 resolution target taken with the developed high magnification system. LEFT: elements 4 to 7; RIGHT: elements 6 and 7 (digital zoom).

3.3 Electron Spectrometer

The electron spectrometer is situated after both the YAG screen and the ICT in the beampath. Simulations were carried out to specify a magnet design that could suitably resolve the electron spectrum up to 200 MeV while complying with both the vertical and horizontal constraints. The magnet assembly was procured from Magnet Sales and Service Limited and characterised in the CLF with a specially developed magnet mapping toolkit. The magnetic field and simulated spectrometer response is shown in Fig. 6. This toolkit, developed at CLF together with colleagues

Figure 10. The magnet mapping toolkit.

from the EPIC collaboration [18], is a useful byproduct of preparing for the experimental campaigns in EPAC. It is being utilised by several groups across CLF to prepare and optimise experimental setups, and will go on to be used in EPAC.

3.4 Probe Beam for Plasma Density Diagnostics

Measurement of the average density of the target does not need high temporal resolution because the expansion of the plasma channel occurs on relatively slow time scales. Therefore, we do not need to compress the probe pulse to sub-100 fs pulses as are often used for plasma imaging. Rather, the probe beam has been designed to use a 5% leakage (~50 mJ) through one of the main beamline mirrors as the beam enters the target area. The 60 mm beam will be telescoped down to approximately 10 mm diameter Imaging with the 0.5 ns duration of the stretched pulse may be blurred, so we plan to use a band-pass filter to reduce the pulse duration. Because of the linear chirp, selection of a reduced bandwidth also reduces the pulse duration.

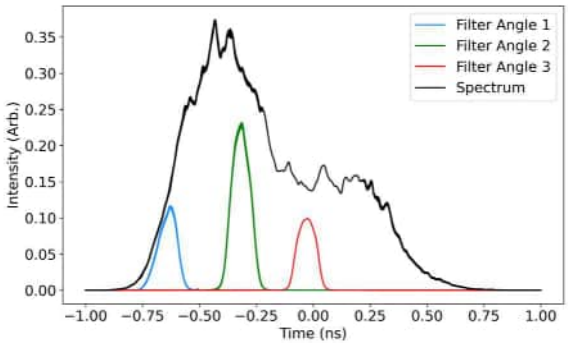

Figure 11. Pulse duration and transmitted energy after selecting specific bandwith of chirped pulse.

The estimated pulse duration produced by using different filters is shown in Fig. 11. For a 5 nm bandwidth filter, up to 10% of the energy incident on the filter will be transmitted, leaving an estimated 5 mJ in the probe pulse at full power, and reducing the pulse duration to 100 ps.

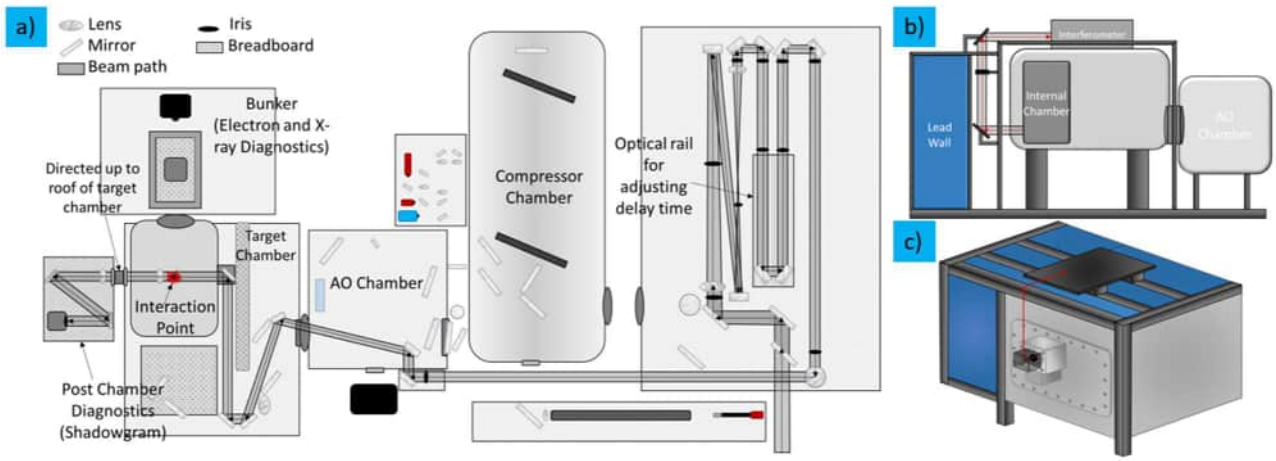

Figure 12. Path of the probe beam in TA2.

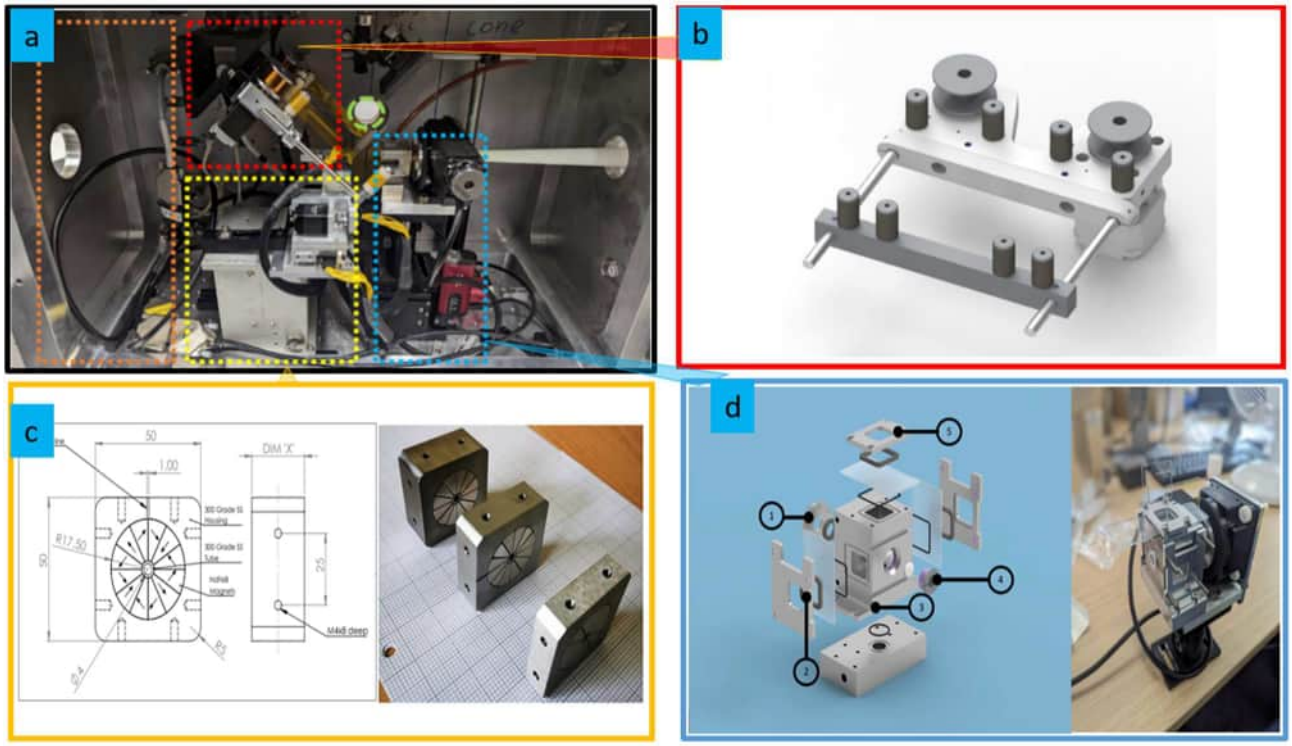

Figure 13. (a) The internal interaction chamber colour coded as follows: orange – space reserved for dielectric streaker; red – kapton tape drive/beam dump **(b)**; yellow – Halbach quadrupole magnet on XYZ translational stage **(c)**; blue – gas-cell (**d):** LEFT: Gas-cell assembly design. 1 – Entrance aperture; 2 – probe beam diagnostics window; 3 – gas-cell volume; 4 – replaceable exit aperture MACOR plate; 5 – top view window. RIGHT: Assembly with a motorized stage to control gas-cell length.

Once the probe pulse is the correct size and duration, it will be directed into the AO chamber. From there it will pass into the interaction chamber and through the gas cell transversely.

After the gas cell, it will be transported to the probe beam diagnostics breadboard, located above the target chamber due to the thick lead shielding that will encase the chamber. The beam will be split into two paths: one to be used for building a shadowgraphy image of the plasma, and the other to pass through a constructed Mach-Zehnder interferometer for a plasma density measurement, based on the phase shift. We expect that a plasma density of 1 x 10^{17} cm^{-3} can be measured with these diagnostics.

4. LWFA Control and Shaping

To progress from LWFA R&D to a fully functioning beamline suitable for applications using the laser-driven secondary sources, it is important to understand what effective mechanisms require controlling, and how to effectively manipulate the electron beam. We will investigate the possibilities of shaping the produced electron beam by manipulation of a variety of factors, including over plasma length (gas cell length), gas pressure, magnetic optical system and dielectric wakefield. We will also explore the potential influence of a tape drive system on electron bunch quality.

4. 1 Gas-Cell Design

To control the plasma density and profile we have designed a custom gas-cell, maintaining the flexibility of the design in Ref. [2, 14] to control the lens and simplify replacing parts etc.

As a source of wakefields, TA2 has a custom designed gas-cell. The overarching aim for the design was to ensure easy maintenance of the cell, since laser jitter can cause significant damage to the exit aperture of the cell and blackening of the probe beam windows from debris, especially operating at 5 Hz repetition rate. The main components of the new design are highlighted in Fig. 13 (d). The slides for the probe beam windows and the top of the cell are standard microscopic glasses. These windows can be replaced simply on a daily basis without removing the gas-cell from the chamber, thus keeping electron beam line alignment consistent throughout the experiment. The exit aperture is made of MACOR plate with a 100µm hole, which is glued into the grub screw construction. The grub screw, together with MACOR plate, will be replaced as a part of the maintenance procedure. The gas-cell will be filled with helium doped with 1% nitrogen to allow for ionization injection. The front aperture could translate to vary the cell length in the range of 0–10 mm. The electron density is expected to be more than 5 × 10^{18} cm^{-3}.

During TA2 operation, the plasma source will be placed in a separate volume within the main target chamber and will be pumped directly by a separate roughing pump (see Fig. 1), the same arrangement that was used in Ref. [2]. The main benefit of differential pumping is the protection it provides for the expensive optics and the gratings in the compressor chamber from the by-product of laser-gas interactions.

4. 2 Halbach Magnets for Beam Focusing

Several beamline configurations for different electron beam energy modes are being designed for EPAC by ASTeC [19]. To allow for adjustment of the beamline for variable energy modes, a set of permanent Halbach quadrupoles will be installed. Because of time constraints, electron focusing components are generally not used on Gemini experiments, thus the test beamline provides an opportunity to understand any unforeseen peculiarities of LWFA beam control using Halbach magnets. Magnets procured for TA2 are shown in Fig. 13 (c) and designed to effectively collimate a beam of 50 -70 MeV. Magnets which are being designed for EPAC are shown in Fig. 14 and described in Ref. [20].

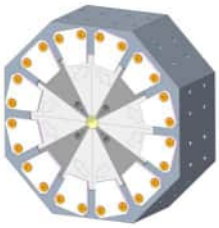

Table 1: Quadrupole Specification.

Peak gradient	≈ 500 T/m
Maximum length	50 mm
Integrated gradient	> 25 T
Internal radius	4 mm
1% good gradient radius	≈ 2 mm
0.1% good gradient radius	≈ 1 mm
Magnetic centre variation	20 μm full range
Peak gradient variation	1% full range

Figure 14. Halbach permanent quadrupoles designed for EPAC. The magnetic blocks have been purchased from VacuumSchmelze GmbH and assembly is underway at ASTeC.

4.3 Dielectric Streaking

Another objective of the testing in TA2 is to develop new diagnostic techniques for ultrashort (~ 10 fs) electron bunches. While the longitudinal profile can be indirectly measured by characterizing transition radiation from a foil [21], there is currently no established method for directly measuring the bunch duration in this regime. A proposal by ASTeC for overcoming the challenges of an ultrashort bunch is to position a dielectric streaker next to the beam propagation, in the way that beam is passed off-axis through a dielectric lined waveguide. This imparts a kick to the electrons that increases from the head to the tail of the bunch and can be observed on a downstream screen. We plan to test this diagnostic using ~50 MeV electron beams in TA2.

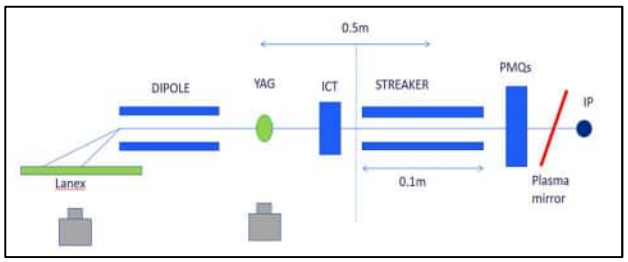

Figure 15. Schematic of the LWFA arrangement for testing the permanent magnet quadrupoles (PMQs) and the dielectric streaker. The streak is measured on the YAG screen and the energy spectrum on the Gadox screen. An integrating current transformer is used to measure the beam charge.

4.4 Tape Drive for Laser Beam Dump

For experiments designed in TA2, the tape-drive will serve mainly as a beam dump, to prevent the remaining laser beam energy (only 10% of laser energy will be deposited for the plasma formation) from propagating though the beam line. We designed a more compact version of the CLF tape design to fit within the spatial constraints of TA2, a render of the new design is shown in Fig. 13 (b). To operate at the higher repetition rate of 5 Hz, the tape is driven continuously, and it was necessary to move towards in-vacuum motors to prevent overheating. A high torque can be maintained using vacuum compatible stepper motors AML-D35.1. This motor will permit 75 mNm in 200 steps per rotation mode. These are connected to a custom-designed motor controller, which is in turn connected to the EPICS IOC through a Modbus interface. The EPICS connection will be used to provide a motor status to the front-end control system, creating a feedback system that allows termination of the laser in case of motor failure, thus preventing damage to diagnostic equipment. During experimental campaigns at TA2, the optimal mechanisms for the tape drive system operation will be researched at 5Hz and necessary improvements will be identified to be deployed for EPAC.

5 Conclusions

We have outlined here our progress towards prototyping experiments to address some of the concerns surrounding increasing the laser repetition rate, in order to minimize the risk of the EPAC project. A combination of software and engineering improvements paired with emerging machine learning techniques should lead to the production of stable, high-quality laser-driven secondary sources.

Acknowledgements

We acknowledge support from all Gemini, Target Fabrication, Mechanical and Electrical engineering teams, as well as our collaborators from ASTeC and EPIC.

References

[1] Symes, D. R., et al, Proposed Target Area 2 work-plan in preparation for EPAC. CLF annual report (2022), https://www.clf.stfc.ac.uk/Pages/Annual-Report-2021-22.aspx

[2] Shalloo, R.J., Dann, S.J.D., Gruse, JN. *et al.* Automation and control of laser wakefield accelerators using Bayesian optimization. *Nat Commun* **11**, 6355 (2020), https://doi.org/10.1038/s41467-020-20245-6

[3] Jalas, S., Kirchen, M., Messner, P. *et al.* Bayesian Optimization of a Laser-Plasma Accelerator, Phys. Rev. Lett. **126**, 10 (2021), https://link.aps.org/doi/10.1103/PhysRevLett.126.104801

[4] Kirchen M., et al., Optimal Beam Loading in a Laser-Plasma Accelerator, Phys. Rev. Lett. **126**, 174801 (2021).

[5] Dazzler, Dazzler - Ultrafast pulse shaper - Fastlite

[6] WaveTune, WAVETUNE Adaptive Optics software | Imagine Optic (imagine-optic.com)

[7] Maier, A. R., "Decoding Sources of Energy Variability in a Laser-Plasma Accelerator", Physical Review X, vol. 10, no. 3, 2020. doi:10.1103/PhysRevX.10.031039.

[8] Bohlen, S., et al. "Stability of ionization-injection-based laser-plasma accelerators." Physical Review Accelerators and Beams 25.3 (2022): 031301. https://arxiv.org/abs/2203.00561

[9] Downer, M. C., et al, Diagnostics for plasma-based electron accelerators, Reviews of Modern Physics, vol. 90, no. 3, 2018. https://doi:10.1103/RevModPhys.90.035002

[10] Liu, H., et al., Cherenkov radiation-based optical fibre diagnostics of fast electrons generated in intense laser-plasma interactions. Review of Scientific Instruments. ISSN 1089-7623, 2018, https://doi.org/10.1063/1.5024872

[11] Bergoz Instrumentation, https://www.bergoz.com/

[12] Nakamura, K., Pico-coulomb charge measured at BELLA to percent-level precision using a Turbo-ICT, Plasma Physics and Controlled Fusion, vol. 58, no. 3, 2016. http://dx.doi.org/10.1088/0741-3335/58/3/034010

[13] EPICS. (n.d.). EPICS - Experimental Physics and Industrial Control System. Retrieved from https://epics-control.org

[14] Dann, S., et al., Laser wakefield acceleration with active feedback at 5 Hz. Physical Review Accelerators and Beams. 22. 10.1103/PhysRevAccelBeams.22.041303.

[15] Albert, F., et al. Characterization and applications of a tunable, laser-based, Mev-class Compton-scattering x-ray source. Phys. Rev. ST Accel. Beams 13, 070704. https://doi.org/10.1103/PhysRevSTAB.13.070704 (2010).

[16] Jing, T., Goodman, C., Cho, G., Drewery, J., Hong, W., Lee, H., et al. (1993). Evaluation of a structured cesium iodide film for radiation imaging purposes. Nuclear Science Symposium and Medical Imaging Conference, 1993., 1993 IEEE Conference Record, 3, 1878-1882.

[17] CRYTUR, https://www.crytur.cz/materials/yagce/

[18] EPIC collaboration, https://www.epic-innovation.org

[19] Muratori B., et al., The EPAC electron transport beamline - physics considerations and design, 14th International Particle Accelerator Conference, Venice, Italy. doi:10.18429/JacoW-IPAC2023-TUPA105

[20] Thomson N., et al., High gradient hybrid Halbach quadrupoles with a novel 3-bit gradient tuning system, 14th International Particle Accelerator Conference, Venice, Italy. doi: 10.18429/JACoW-IPAC2023-WEPM031

[21] Schmidt, B., Wesch, S., Kövener, T., Behrens, C., Hass, E., Casalbuoni, S. and Schmüser, P., 2018. Longitudinal bunch diagnostics using coherent transition radiation spectroscopy. arXiv preprint arXiv:1803.00608.